Optica Applicata, Vol. XXXV, No. 3, 2005

Properties and origin of oval defects in epitaxial structures grown by molecular beam epitaxy

ANNA SZERLING, KAMIL KOSIEL, ANNA WÓJCIK-JEDLIŃSKA,
MARIUSZ PŁUSKA, MACIEJ BUGAJSKI

Institute of Electron Technology, al. Lotników 32/46, 02-668 Warszawa, Poland

A class of macroscopic, so-called oval defects, which may be found in an epitaxial A^3B^5 materials grown by molecular beam epitaxy (MBE) technique, is studied in this paper. The investigations were performed on the structures containing (Al)GaAs or InGaAs layers. The geometry, morphology as well as the optical properties of defects were studied by different experimental methods, like spatially resolved photoluminescence (SRPL), scanning electron microscopy (SEM) and cathodoluminescence (CL). The conclusions are drawn as to the sources of defects and conditions of their appearance.

Keywords: oval defects, A^3B^5, molecular beam epitaxy (MBE), spectrally resolved photoluminescence, scanning electron microscopy (SEM), cathodoluminescence.

1. Introduction

Among the defects found in A^3B^5 crystalline materials the class of so called oval defects is characteristic for layers grown by molecular beam epitaxy (MBE). For example, the so-called oval defects.

The presence of oval defects limits the use of MBE technique degrading both volume and surface uniformity of chemical properties of the epitaxial material, creating problems at the device processing stage, and being a serious obstacle to device integration and fabrication of laser matrices. For this reason it is necessary to know their origin in order to eliminate these disadvantageous effects, by means of providing the appropriate conditions of the crystallisation process. That is why sources of oval defects and methods of their elimination are studied in many laboratories.

Oval defects have been known in MBE grown layers for more than 20 years and many proposals concerning reduction of the level of the defects were formulated at laboratories around the world. Every technological environment, however, has its particular features and that is why it is usually necessary to perform a complete

investigation of the specific issues related to the particular growth system and to compare results with the data published.

Oval defects have characteristic shape, highlighted by their name. They are typically elongated in ⟨110⟩ direction when layers are deposited on (001) oriented crystalline substrates. Their size is up to 50 μm and the surface density varies in the range of 10^2–10^5 cm^{-2} [1–3], depending on the epitaxial layer thickness, growth conditions and the purity of the substrate surface and of epitaxy environment. Oval defects, in most cases being a kind of big three dimensional islands, should, however, be distinguished from other type of noncoherent islands – extra defected by so-called misfit and edge dislocations. The latter may be created as a result of long lasting growth of lattice mismatched layer, continuing the early stages of Stranski–Krastanow or Volmer–Weber growth modes. Such islands are objects observed in materials grown by means of a variety of epitaxial techniques.

Here, we present certain types of oval defects observed in A^3B^5 materials containing (Al)GaAs or InGaAs layers, grown by means of MBE. After preliminary inspection by optical microscopy (also with Nomarski contrast) we have studied properties of our structures by means of scanning electron microscopy (SEM), cathodoluminescence (CL) and spatially resolved photoluminescence (SRPL) mapping.

Defects observed in the structures grown in our MBE laboratory are rather rare phenomena. However, the growth of complicated nanoelectronic structures requires the application of a wide range of growth conditions, which causes the danger of oval defect appearance. Their elimination is difficult, especially if the reason of their formation is not absolutely clear. In order to fully understand these processes it is essential to perform a comprehensive investigation of oval defects by means of different experimental techniques. The earlier works concerning the oval defects done in Institute of Electron Technology (IET) [2] were restricted mainly to optical microscope inspection of the grown structures and were directed towards seeking a correlation between growth conditions and defect density. In the present work, we take advantage of SEM, CL and SRPL mapping, the techniques which give more insight in the individual defect properties and can eventually help to clarify defect origin. Combining the results of our investigation with world literature data we make conclusions concerning main sources of oval defects in our epitaxial technology.

2. Types and possible sources of oval defects

Various categorizations of oval defects were proposed by authors working in the field. However, taking into account sources of oval defects, we may distinguish two main defect groups:

– objects formed as a result of contamination by particles coming from parts of a reaction (evaporation) chamber other than effusion cells, *e.g.*, reactor walls or a substrate holder, and particles contaminating surface of a crystalline substrate before placing it in a reactor, for example, the particles present in the laboratory environment;

– objects created as a result of pollution by matter originating from effusion cells.

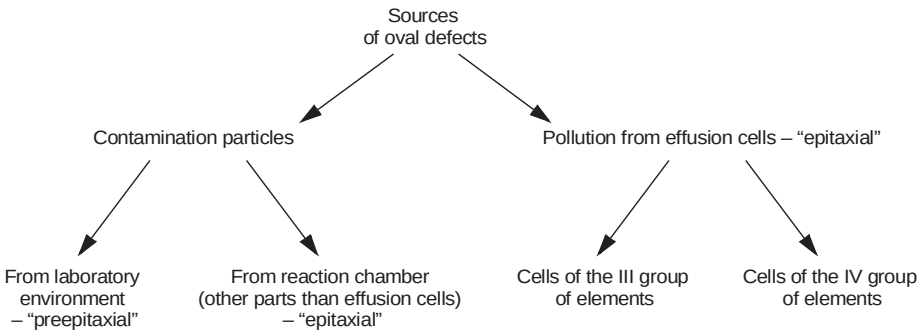

Fig. 1. Sources of oval defects.

We may also notice that, on the other hand, it is practical to divide these sources into two groups:

– "preepitaxial", *i.e.*, present in laboratory environment (outside the reaction chamber);

– "epitaxial", *i.e.*, present in epitaxy environment (in a reaction chamber).

The sources of oval defects are schematically presented in Fig. 1. It has to be emphasized that the scheme presented is rather simplified.

2.1. Oval defects not related to effusion cells

"Preepitaxial" contamination particles may be liquid or solid and may appear as a residual polishing dust, traces of reagents used for chemical treatment of crystal wafers or a GaAs dust remaining after the operation of cleaving the crystalline substrate. "Epitaxial" particles of contamination from walls of evaporation chamber or substrate holder are solid dusts of recrystallised arsenic, or crystallised arsenides. It is hard to distinguish between the "preepitaxial" and "epitaxial" defects caused by the above sources of pollution if the question is not solved by cross sectional transmission electron microscopy of the epitaxial material. A characteristic morphological property of defects of these types appears as an oval "spike" accompanied by a pit or a crater

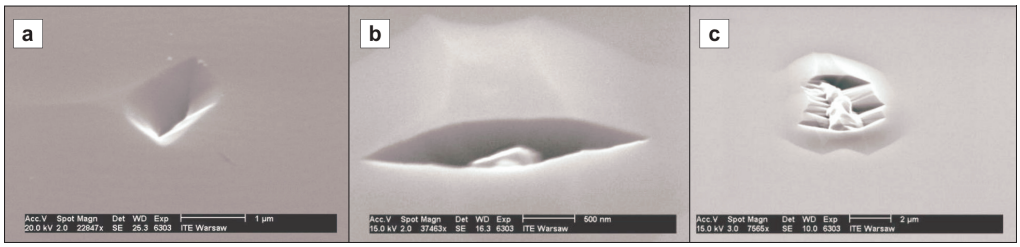

Fig. 2. Scanning electron micrographs showing: (**a**) a pit on the surface of the top epitaxial layer of the $Al_{0.3}Ga_{0.7}As/GaAs$ structure, related to a hole in the crystalline substrate, (**b** and **c**) oval defects with "spike" deep-seated in the pit caused by a particle of contamination (the surface of AlGaAs/InGaAs/GaAs structure).

[1, 4, 5], which is shown in Fig. 2**a**. Reduction of the density of such defects is connected with taking care of sufficient purity of crystalline substrates, laboratory atmosphere and MBE growth chamber. The above-mentioned "spikes" indicate the difference between these defects and pits in the epitaxial layer surface, being the result of holes in the substrate which are present there before the deposition process (see Fig. 2**b** and **c**).

2.2. Oval defects related to effusion cells

Though we observe some oval defects not related to effusion cells and some pits (like in Fig. 2**b**, **c** and **a**, respectively) in our epitaxially grown A^3B^5 material, the most frequently found defects are of different nature. We have found them to be the effusion cell related defects.

According to some hypotheses, small gallium droplets "spitting" from the Ga effusion cell on the surface of epitaxially growing crystal, play a crucial role in the process of oval defects formation [1, 4–7]. The gallium condensed at the orifice of the gallium crucible rolls back and splashes into the gallium melt, being the cause of "spitting". The properties of Ga related oval defects formed in such a way depend on the size of falling gallium droplets [1, 4–7]. The metallic matter of a gallium droplet makes the basis of the defect.

In accordance with another hypothesis, gallium oxides related to Ga effusion cell [1, 4–8] are of primary importance in the defect formation process. Gallium suboxide (Ga_2O) is formed in the Ga crucible. The adequate chemical reactions of Ga_2O formation [1, 4–8] are presented below:

$$Ga_2O_3 + 4Ga \rightarrow 3Ga_2O$$

or

$$Ga_2O_3 + 4GaAs \rightarrow 3Ga_2O + As_4$$

or

$$2C + Ga_2O_3 \rightarrow Ga_2O + 2CO$$

The last equation presents the reaction with residual carbon.

Gallium suboxide comes together with the gallium droplets or alternatively, because it is volatile, it is evaporated from the Ga effusion cell. As a result of chemical reaction of gallium suboxide on the surface of the growing crystal, gallium trioxide (Ga_2O_3) and gallium are created:

$$3Ga_2O \rightarrow Ga_2O_3 + 4Ga$$

Gallium (and according to other hypothesis Ga_2O_3) is the basis of the defect.

As a result of the falling of relatively small gallium droplets on the surface of growing crystal, the Ga cell related defects without a core are said to be formed. Droplets wet the crystalline surface and cause locally faster growth of the crystal.

In contrast to the defects created by small Ga droplets, oval defects with a core are suspected to be formed on the basis of relatively big metal droplets. Part of such a big droplet does not wet the crystal surface and makes a nucleus of the defect core.

Some authors also formulate a hypothesis concerning the existence of As cell related defects whose source, *i.e.*, arsenic oxides, are present in the arsenic cell.

The studies so far have concentrated basically on the homoepitaxial GaAs layers, however, the problems discussed relate to every Ga containing epitaxial layer [9]. Though maximum attention was devoted to the influence of Ga effusion cell [1, 4–8], we think that other effusion cells of the third group elements, which are used during the growth of more complex structures should also be considered as a possible source of oval defects. The data found in other works [3] seem to confirm this idea.

3. Experimental

All materials studied were grown by solid state MBE using Riber 32P machine, equipped with ABN 135L evaporation cells and As_4 source. Epilayers were deposited on (100)±0.1° oriented GaAs crystalline substrates, n^+ or semi-insulating (SI), supplied by AXT.

Our studies concern three types of epitaxial material: homoepitaxial approximately 1 μm thick GaAs layers, heterostructures composed of $Al_{0.3}Ga_{0.7}As$ layer deposited on top of the GaAs buffer layer (both layers approximately 1 μm thick) and heterostructures with nominally 8 nm thick $In_{0.2}Ga_{0.8}As$ strained layer embedded in the $Al_{0.3}Ga_{0.7}As$/GaAs stack of macroscopically thick layers.

We studied some selected oval defect individuals which seem to be typical of population in our materials. That is why we focused on the defects which seem to be related to effusion cells. A set of characterisation methods presented below was applied to them.

We have used room temperature SRPL to investigate our structures. The exciting laser beam was focused on the sample by microscope objective, providing the spot diameter of the order of 1 μm (this value is determined by diffraction limit of objective). The penetration depth of the laser beam should be great enough to achieve the optically active region of multilayer structure. In most cases we have used He-Ne or Ar^+ lasers, depending on the kind of structure investigated.

The samples were placed on the stage integrated with scanning module; *X*-*Y* stages combined with two mechanical encoders. The measurement points formed a square mesh covering the investigated area on the sample. The scanning step may even be less than 1 μm. The LN_2 cooled CCD camera collects the whole PL spectrum for each point examined. Each spectrum was numerically processed and only the main signatures of the PL feature were saved, *i.e.*, the integrated PL intensity and the spectral position of maximum. In this way, we have obtained a set of maps with characteristic parameters of the area under investigation.

All scanning electron micrographs of defects have been performed at room temperature using Philips XL30 Scanning Electron Microscope. Two modes of

detection were utilized; detection of secondary electrons and CL (the last one being monochromatic as well as panchromatic). We have used the mode of detection of secondary electrons to visualize the geometry of defects. CL investigations were performed by using the MonoCL (Oxford Instruments) set consisting of monochromator and photomultiplier. In most cases the energy of electron beam, which excited structures, was equal to 30 keV.

4. Results and discussion

4.1. GaAs homoepitaxial layers

Oval defects found on the surfaces of GaAs layers exhibit a broad range of shapes, so we can find "simple" as well as more "complicated " individuals. The latter may be described as having their polyhedral and approximately spherical parts. The scanning electron micrographs present their possible shapes (see Fig. 3).

As a rule the oval defects in GaAs are optically degraded. This fact is seen in the panchromatic CL images (Fig. 4**a**, **c**), where the regions of the defects are dark. The same behaviour is also observed on the PL intensity maps obtained by SRPL technique (Fig. 4**b**, **c**). A precise investigation of the defect individuals shows that the isointensity lines of luminescence in the area of oval defect exist (Fig. 4**d**, inset). The lack of luminescence is found in the central part of defect.

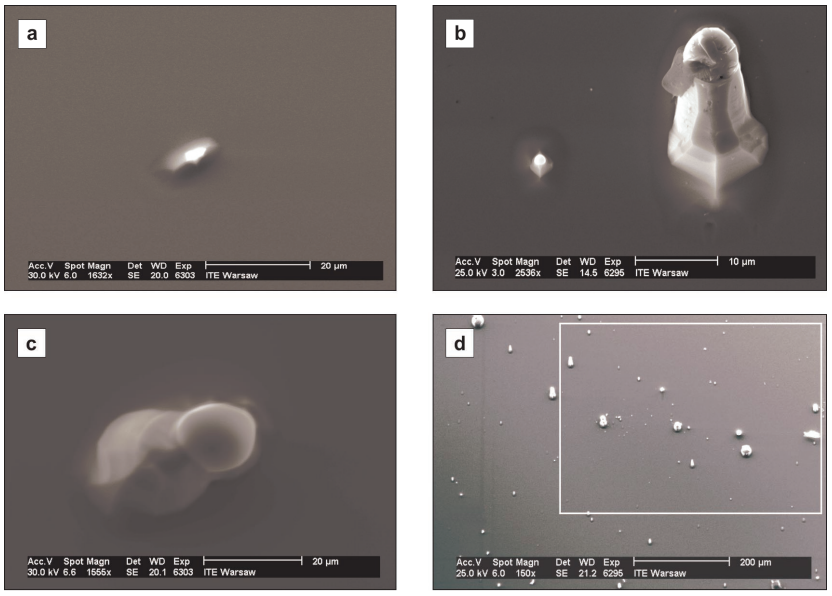

Fig. 3. Scanning electron micrographs of oval defects found on the surface of GaAs homoepitaxial layer. Selected individual defects – **a**, **b**, **c** (photos **a**, **b** and **c** should be compared with Fig. 5**l**, Fig. 4**c**, **d** and with Fig. 5**a**–**k**, respectively); a group of defects – **d** (the frame includes the same group of oval defects as the frame in the Fig. 4**b**).

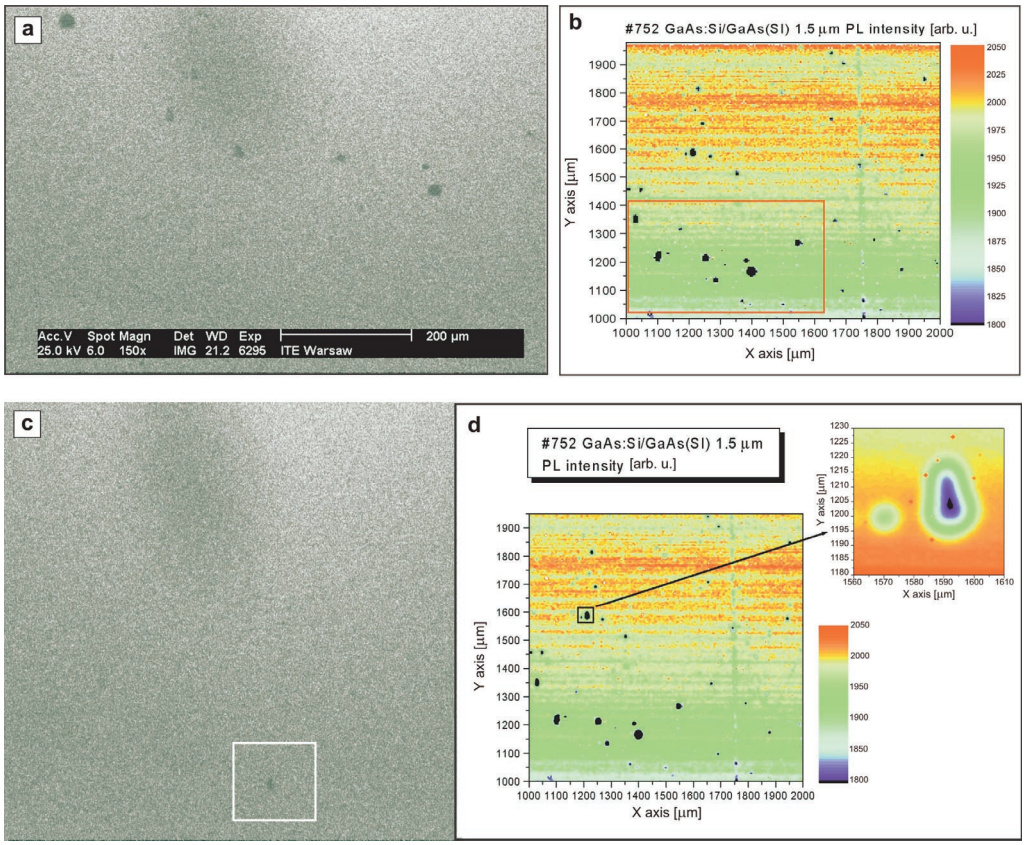

Fig. 4. Panchromatic CL images (**a**, **c**) and room temperature SRPL intensity maps (**b**, **d**) of the surface of GaAs homoepitaxial layer. The area of (**a**) is the same as in Fig. 3(**d**). The frame in (**b**) includes the same group of oval defects as the frame in Fig. 3(**d**). The frame in (**c**) includes the pair of defects presented in the inset of (**d**) and in the micrograph, in Fig. 3**b**.

As was mentioned above, the majority of oval defects shows optical inactivity in the case of panchromatic CL. These individuals present also the expected inactivity in monochromatic CL, which was studied for a file of defects for wavelengths in the range of 820–910 nm. This is particularly true for the wavelength of 870 nm, which corresponds to gallium arsenide energy bandgap (Fig. 5**l**). There are, however, some defect individuals showing CL optical activity in fragments of their bodies with maximum intensity for 870 nm, simultaneously manifesting optical degeneration for CL from the rest of their volume (Fig. 5**a**–**j**). What is more, the observed CL from optically active part of defect is much more intensive than the 870 nm CL generated in the surrounding area. The behaviour of such defects in PL measurement is quite different, that is, the configuration patterns of optical activity for these two mechanisms of stimulation (by means of laser beam or electron beam) do not overlap (Fig. 5**k**).

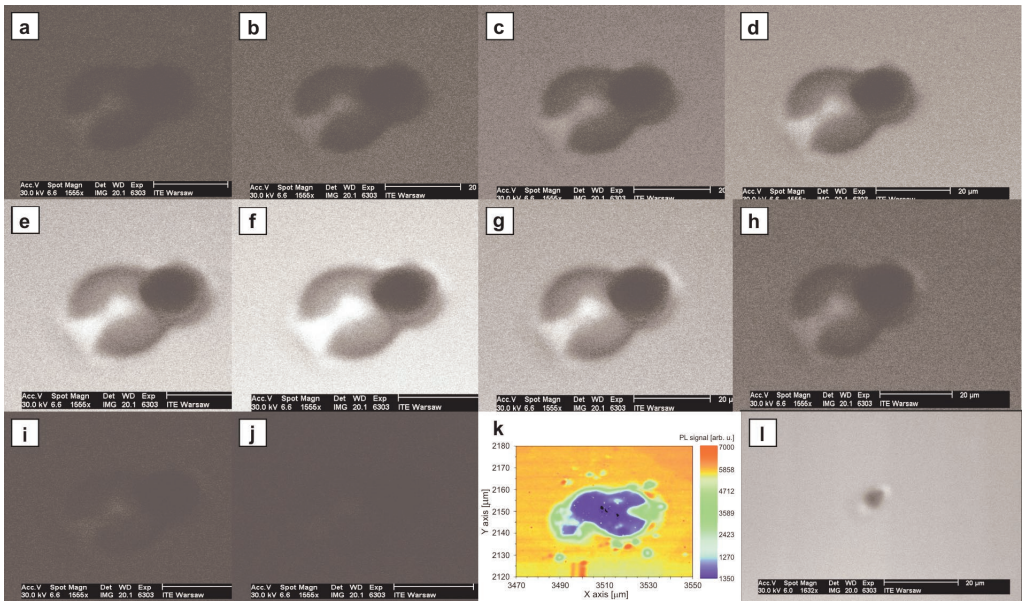

Fig. 5. Collection of monochromatic CL images (**a**–**j**) for the oval defect found on the GaAs surface. The file of pictures corresponds to the wavelength region from 820 nm (**a**) to 910 nm (**j**), with the monotonic change of wavelength from (**a**) to (**j**) with the step of 10 nm; (**k**) the SRPL intensity map for the same defect – in comparison with figures (**a**–**j**) this picture is turned in the plane of the page through an angle of about 180°. The same individual is seen in the micrograph in Fig. 3**c**; (**l**) monochromatic 870 nm CL image for defect shown also in Fig. 3**a**.

The room temperature PL wavelength in the investigated areas of homoepitaxial GaAs layers was 870 nm, without any changes of value for the sake of presence of oval defects. That is why we make an assumption that oval defects in GaAs do not incorporate any strain into the crystal lattice and hence do not change the energy bandgap of the semiconductor.

4.2. $Al_{0.3}Ga_{0.7}As$/GaAs heterostructures

As opposed to oval defects found in homoepitaxial GaAs these ones characteristic of $Al_{0.3}Ga_{0.7}As$ layers deposited on GaAs present optical activity in panchromatic CL measurement, at least in parts of their bodies Fig. 6**b**. The CL intensity from defects is even higher than for their surroundings.

Typical of the majority of defects found in $Al_{0.3}Ga_{0.7}As$ layers is a specific structure. They may be described, using simplification, as being composed of three regions when their optical properties are taken into account: optically active centre and outer ring (both of higher intensity than the surroundings of the defect, especially the centre) and optically inactive (degraded in comparison with the surrounding) inner ring placed between these two previously introduced elements (Fig. 7**a**, **b**). The PL

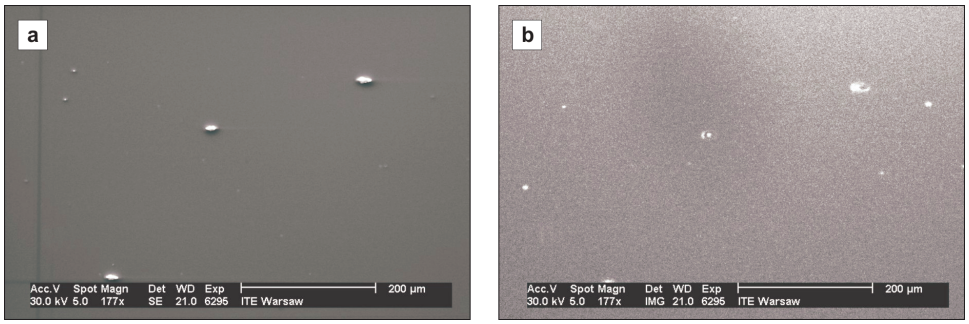

Fig. 6. Surface of $Al_{0.3}Ga_{0.7}As$ layer deposited on GaAs: scanning electron micrograph (**a**), panchromatic CL image (**b**).

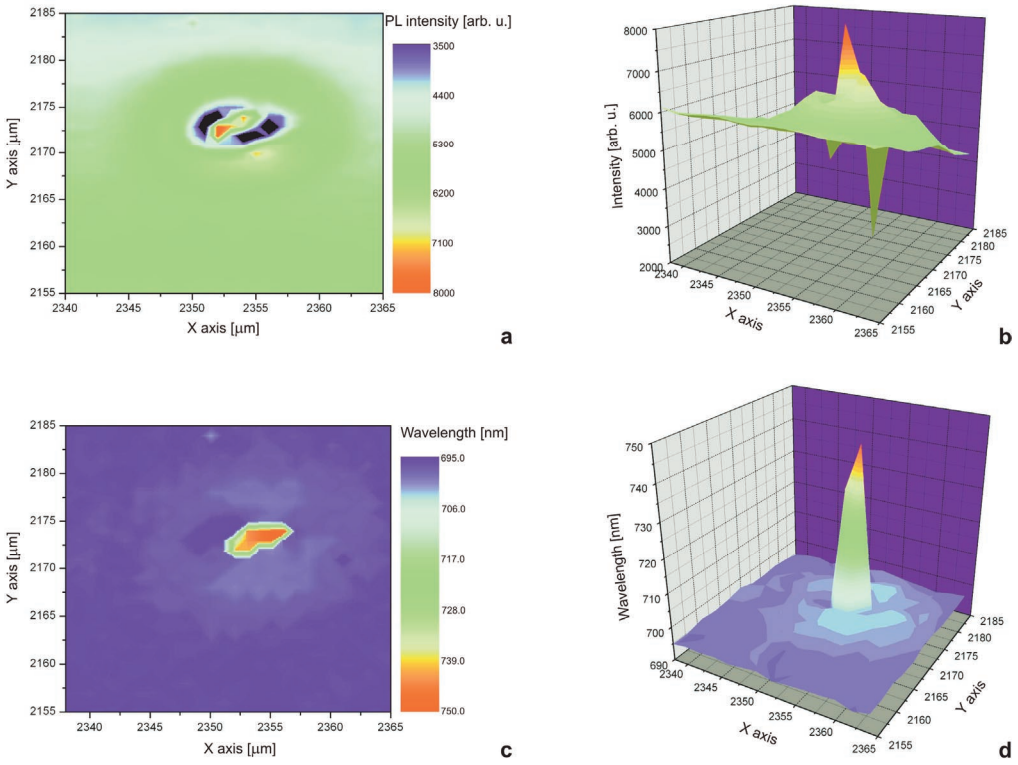

Fig. 7. SRPL intensity (**a**, **b**) and wavelength (**c**, **d**) maps of the oval defect selected from the surface of $Al_{0.3}Ga_{0.7}As/GaAs$ structure (**a**, **c** – planar maps; **b**, **d** – three dimensional maps).

wavelength characteristic of the centre and of the outer ring is a few tens of nanometers and nearly ten nanometers, respectively, longer than for the not defected surface (Fig. 7**c**, **d**). The model of the structure of the defect, which is suggested above by PL data, is confirmed by the collection of monochromatic CL micrographs (Fig. 8). It is

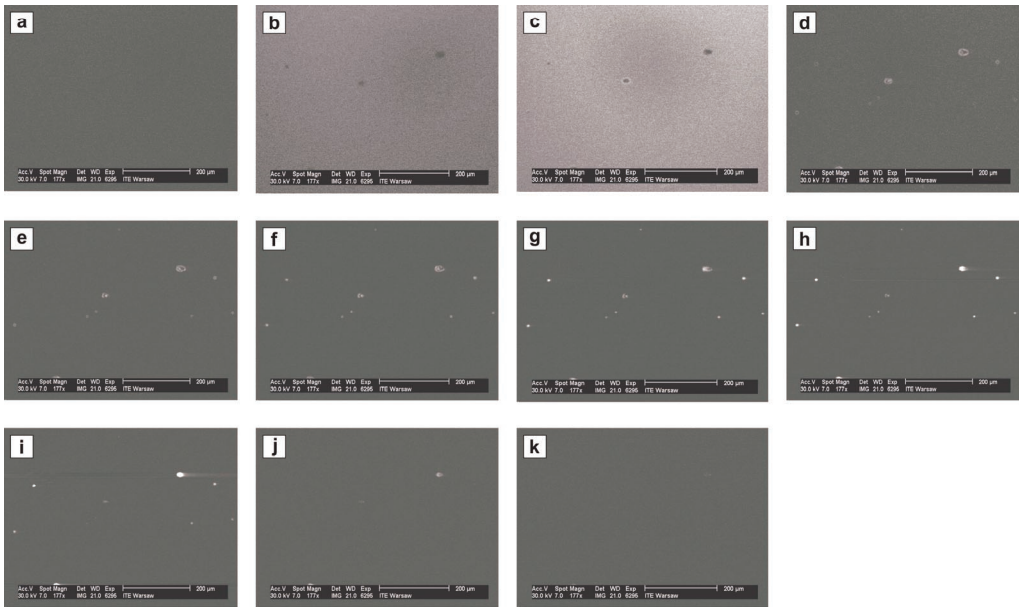

Fig. 8. Collection of monochromatic CL images for the oval defect found on the surface of $Al_{0.3}Ga_{0.7}As/GaAs$ structure. The file of pictures corresponds to the wavelength region from 650 nm (**a**) to 900 nm (**k**), with the monotonic change of wavelength from (**a**) to (**k**) with the step of 25 nm.

clearly seen that three main parts of each defect body present CL activity for different wavelengths.

Because we have made an assumption concerning the lack of defect derivative lattice strain in GaAs and taking into account the lattice matching in AlGaAs/GaAs system, here we also suggest the absence of strain in AlGaAs and propose a hypothesis that the defect related PL wavelength distribution in the layer is a result of non-uniform chemical composition.

Taking into consideration this fact we can say that the composition of the centre and the outer ring of the representative oval defect is $Al_{0.04}Ga_{0.96}As$ and $Al_{0.24}Ga_{0.76}As$, respectively. That is, these regions, and especially strongly the centre, are enriched in gallium. This confirms the hypothesis concerning the gallium cell related origin of oval defects. Because we have not found any traces of defects related to aluminum cell, we state that the gallium cell origin of oval defects is the truth also for GaAs layers.

4.3. $In_{0.2}Ga_{0.8}As/Al_{0.3}Ga_{0.7}As/GaAs$ heterostructures

The PL intensity from oval defects of $In_{0.2}Ga_{0.8}As/Al_{0.3}Ga_{0.7}As/GaAs$ epitaxial structures is higher than for their surroundings (Fig. 9**a**). This makes a difference between structures containing InGaAs layers and simple homoepitaxial GaAs. We could not find, however, any structure of the defects unlike for $Al_{0.3}Ga_{0.7}As/GaAs$ structure. The defects may be divided into two groups, if the PL wavelength

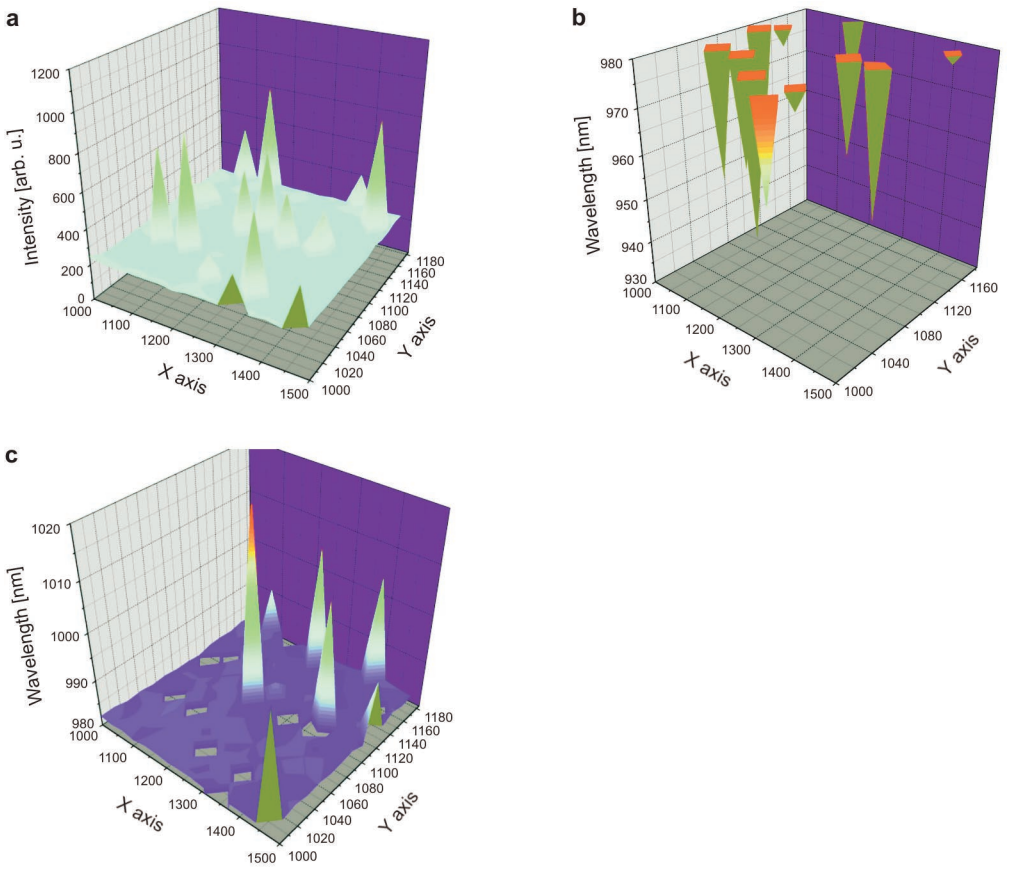

Fig. 9. Three dimensional SRPL maps of the fragment of the surface of $In_{0.2}Ga_{0.8}As/Al_{0.3}Ga_{0.7}As/GaAs$ heterostructure: intensity (**a**), wavelength – two constituent maps (**b**, **c**).

characteristic of them is taken into account. There are defects emitting shorter or longer wavelength in the $In_{0.2}Ga_{0.8}As/Al_{0.3}Ga_{0.7}As/GaAs$ structures. The first ones (of about 1.5 times greater density) are supposed to be related to the gallium effusion cell. The shorter emission wavelength may be the result of smaller indium concentration in the area where the gallium rich defect exists. The second ones are thought to be related to the indium effusion cell. The longer emission wavelength may be the result of higher indium concentration in the area where defect of this type exists. In oval defects of the two types mentioned above the composition deviations (in the content of the III group of elements) reach several percent.

5. Conclusions

We have accomplished the study of MBE grown A^3B^5 structures by means of scanning electron microscopy, cathodoluminescence, and spatially resolved photoluminescence.

We studied GaAs/GaAs, $Al_{0.3}Ga_{0.7}As$/GaAs as well as $In_{0.2}Ga_{0.8}As/Al_{0.3}Ga_{0.7}As$/GaAs structures.

We have observed the presence of some kinds of oval defects. Morphology, geometry and optical properties of the defects have been determined. Moreover, the most probable sources of the defects have been indicated.

The most frequent oval defects are cell related ones. Non effusion cell related defects occur relatively rarely.

Among the cell related defects we found some individuals with optically degraded areas. In GaAs/GaAs and $Al_{0.3}Ga_{0.7}As$/GaAs structures the population of cell related defects contains only the Ga related ones. The Ga cell related defects found on the surface of $Al_{0.3}Ga_{0.7}As$ present "ring-like" structure with characteristic distribution of chemical composition, different from the defects found in homoepitaxial GaAs. When defects of GaAs are as a rule optically degraded, there are parts of defects of $Al_{0.3}Ga_{0.7}As$ that are even more optically active than their surroundings.

In $In_{0.2}Ga_{0.8}As/Al_{0.3}Ga_{0.7}As$/GaAs structures two kinds of oval defects are found. They are supposed to be gallium cell related and indium cell related ones. They present higher optical activity than their surroundings.

Acknowledgement – This work was partially supported by the Polish State Committee for Scientific Research under grant no. 3 T11B 045 27.

References

[1] CHAND N., CHU S.N.G., *Comprehensive study and methods of elimination of oval defects in MBE-GaAs*, Journal of Crystal Growth **104**(2), 1990, pp. 485–97.

[2] KLIMA K., KANIEWSKA M., REGIŃSKI K., KANIEWSKI J., *Oval defects in the MBE grown AlGaAs/InGaAs/GaAs and InGaAs/GaAs structures*, Crystal Research and Technology **34**(5-6), 1999, pp. 683–7.

[3] RUSSELL-HARRIOTT J.J., ZOU J., MOON A.R., COCKAYNE D.J.H., USHER B.F., *Investigation of oval defects in InGaAs/GaAs strained-layer heterostructures using cathodoluminescence and wavelength dispersive spectroscopy*, Applied Physics Letters **73**(26), 1998, pp. 3899–901.

[4] KAWADA H., SHIRAYONE S., TAKAHASHI K., *Reduction of surface defects in GaAs layers grown by MBE*, Journal of Crystal Growth **128**(1-4), 1993, pp. 550–6.

[5] MATTESON S., SHIH H.D., *Morphological studies of oval defects in GaAs epitaxial layers grown by molecular beam epitaxy*, Applied Physics Letters **48**(1), 1986, pp. 47–9.

[6] CHAI Y.G., CHOW R., *Source and elimination of oval defects on GaAs films grown by molecular beam epitaxy*, Applied Physics Letters **38**(10), 1981, pp. 796–8.

[7] SHINOHARA M., ITO T., *Thermodynamic study on the origin of oval defects in GaAs grown by molecular-beam epitaxy*, Journal of Applied Physics **65**(11), 1989, pp. 4260–7.

[8] WENG S.-L., *Ga_2O_3: the origin of growth-induced oval defects in GaAs molecular beam epitaxy*, Applied Physics Letters **49**(6), 1986, pp. 345–7.

[9] PAPADOPOULO A.C., ALEXANDRE F., BRESSE J.F., *Characterization of oval defects in molecular beam epitaxy $Ga_{0.7}Al_{0.3}As$ layers by spatially resolved cathodoluminescence*, Applied Physics Letters **52**(3), 1988, pp. 224–6.

Received June 6, 2005